Published online 20 April 2014

Nucleic Acids Research, 2014, Vol. 42, No. 11 ***e90***
doi: 10.1093/nar/gku297

Live-cell imaging of Pol II promoter activity to monitor gene expression with RNA IMAGEtag reporters

Ilchung Shin[1,2,†], Judhajeet Ray[1,2,†], Vinayak Gupta[3], Muslum Ilgu[1,2], Jonathan Beasley[3], Lee Bendickson[1], Samir Mehanovic[4], George A. Kraus[3] and Marit Nilsen-Hamilton[1,2,*]

[1]Ames Laboratory, US Department of Energy, Ames, IA 50011, USA, [2]Roy J. Carver Department of Biochemistry, Biophysics and Molecular Biology, 1210 Molecular Biology Building, Iowa State University, Ames, IA 50011, USA, [3]Department of Chemistry, Iowa State University, Ames, IA 50011, USA and [4]Molecular Express, Inc., Ames, IA 50014, USA

Received September 20, 2013; Revised March 26, 2014; Accepted March 28, 2014

ABSTRACT

We describe a ribonucleic acid (RNA) reporter system for live-cell imaging of gene expression to detect changes in polymerase II activity on individual promoters in individual cells. The reporters use strings of RNA aptamers that constitute IMAGEtags (Intracellular MultiAptamer GEnetic tags) that can be expressed from a promoter of choice. For imaging, the cells are incubated with their ligands that are separately conjugated with one of the FRET pair, Cy3 and Cy5. The IMAGEtags were expressed in yeast from the GAL1, ADH1 or ACT1 promoters. Transcription from all three promoters was imaged in live cells and transcriptional increases from the GAL1 promoter were observed with time after adding galactose. Expression of the IMAGEtags did not affect cell proliferation or endogenous gene expression. Advantages of this method are that no foreign proteins are produced in the cells that could be toxic or otherwise influence the cellular response as they accumulate, the IMAGEtags are short lived and oxygen is not required to generate their signals. The IMAGEtag RNA reporter system provides a means of tracking changes in transcriptional activity in live cells and in real time.

INTRODUCTION

Changes in gene expression are central to most alterations in cellular functions, yet our current means of measuring transcriptional changes in live cells are limited. Mostly indirect measurements of reporter protein levels are used to monitor transcriptional activity. The use of fluorescent reporter proteins allows live-cell imaging, but all protein reporter systems include a significant lag in time between transcriptional initiation and protein appearance (1). Also, the expressed proteins are long-lived and can be toxic or alter behavior of the cells in which they accumulate (2–5). Ribonucleic acid (RNA) reporters can provide a more timely detection of changes in transcription in living cells and leave a smaller footprint on cellular functions.

Two types of transcription reporter systems using RNA elements have, so far, been shown to function in living cells. One utilizes a repeated segment of the bacteriophage RNA protein binding domains and protein-GFP (green fluorescent protein) fusion proteins (such as MS2-GFP) for imaging (6–9). Sensitivity in these systems is limited by the high background fluorescence of the fluorescent fusion proteins, and thus they require sophisticated image analysis to separate the true signal from background noise. To solve this problem, transcription reporters have been developed that bring together split GFPs linked with two different RNA-binding proteins (9,10). However, all methods for monitoring transcription based on protein reporters require that the host cells constitutively express one or more reporter proteins as well as the tagged target RNA, thus limiting their potential application to a broad range of cell types. This is because of the required genetic manipulation, which can result in loss of differentiated functions, particularly of mammalian cells and because the expressed proteins are long-lived and can be toxic to the cells that express them (2–5). The second RNA-based reporter, referred to as Spinach (11), creates a signal by promoting the fluorescence of a GFP fluorophore mimic. We find that this RNA reporter is useful for imaging the transcription products of RNA polymerase III, but is not sufficiently sensitive to enable detection of the lower abundance RNA polymerase II-derived messenger RNAs (mRNAs).

*To whom correspondence should be addressed. Tel: 515-294-9996; Fax: 515-294-0453; Email: marit@iastate.edu
†The authors wish it to be known that, in their opinion, the first two authors should be regarded as Joint First Authors.
Present address:
Ilchung Shin, Narcotic Analysis Division, National Forensic Service, Seoul 158-707, Korea.
Vinayak Gupta, Department of Chemistry, The Scripps Research Institute, Jupiter, FL 33458, USA.

Here we describe an RNA-based reporter, which we call IMAGEtags (Intracellular MultiAptamer GEnetic tags), for imaging polymerase II transcriptional activity in live cells. The IMAGEtags (strings of RNA aptamers) recognize exogenously supplied fluorescent ligands. Increased sensitivity compared with Spinach was achieved by utilizing a Förster resonance energy transfer (FRET) signal for recognition of the aptamer presence. To demonstrate the applicability of this method, we have visualized GAL1, ACT1 and ADH1 promoter activities using IMAGEtags in living yeast cells. This new RNA reporter system enables live-cell imaging of newly transcribed mRNA in response to changes in promoter activity.

MATERIALS AND METHODS

Solutions and reagents

Buffer IC (13.5-mM NaCl, 150-mM KCl, 0.22-mM Na_2HPO_4, 0.44-mM KH_2PO_4, 100-μM $MgSO_4$, 120-nM $CaCl_2$, 120-μM $MgCl_2$, 20-mM HEPES (4-(2-hydroxyethyl)-1-piperazineethanesulfonic acid), pH 7.3 at 24°C), which was formulated to approximate intracellular pH and cation concentrations based on literature reports for these values (12–16), was used to determine binding constants of various aptamer–ligand interactions. Tris buffered saline (TBS: 50-mM Tris-HCl, 150-mM NaCl and pH 7.6) was used in yeast cell imaging studies. Chemical syntheses of ligands and the properties of the synthetic products are found in the Supplementary material (including Supplementary Figures S1–S3).

Yeast and plasmids

Saccharomyces cerevisiae (BY4735, Genotype: MATαade2Δ::hisGhis3Δ200leu2delta0 met15Δ0trp1Δ63ura3Δ0) was cultured in YPD medium (Yeast extract-peptone-dextrose medium). The yeast expression plasmid, pYES2, is a yeast 2-μm plasmid carrying a URA3 marker and a GAL1 promoter for galactose inducible gene expression in *S. cerevisiae*. The pYES2 plasmid was modified to express IMAGEtag reporter RNAs consisting of a series of tandem aptamers (Supplementary Figure S4) with specificities for 2-[[(3-Aminophenyl)methyl]amino]-6-(2,6-dichlorophenyl)-8-methyl-pyrido[2,3-d]pyrimidin-7(8H)-one (PDC) (17) or tobramycin (Supplementary Figure S5). The IMAGEtag sequences were inserted after the GAL1 promoter and a transcriptional start site (sequences in Supplementary Table S2). The GAL1 promoter was replaced with the ACT1 or ADH1 promoters from yeast to generate expression constructs with the 6xPDC IMAGEtags downstream from these constitutive promoters. Plasmids with IMAGEtag reporters were transformed into BY4735 using the Lazy Bones yeast transformation method and selection on SD (synthetic dropout) minus uracil (SD−uracil) plates (18). The IMAGEtags are identified by the number of aptamers per string and the identity of the aptamer in the IMAGEtag. For example, the 5xTOB IMAGEtag contains five tobramycin aptamers each separated by a 4-nucleotide (A_4) linker and the 6xPDC IMAGEtag contains six PDC aptamers separated by a 4-nucleotide (A_4) linker.

FRET image acquisition and analysis

For FRET analysis by sensitized emission, yeast cells were cultured in SD−uracil medium overnight with either 2% glucose or 2% raffinose. The cells were then induced with SD−uracil medium containing 2% galactose and 1% raffinose for the induction period and incubated with the Cy3- and Cy5-modified ligands. Cells were either washed once with TBS or washed and resuspended in SD−uracil with 2% galactose and 1% raffinose. A 30-μl volume was placed on a poly L-lysine-coated cover glass or a poly D-lysine-coated glass bottom culture dish (MatTek). The cells were observed using a Nikon Eclipse 200 or Leica SP5X laser scanning confocal microscope with a 63X objective and immersion oil. Cells were excited by a 568-nm Argon/Krypton laser (Nikon) or a 550-nm (for Cy3); 650-nm (for Cy5) white light laser (WLL, Leica) and images were taken to measure sensitized emission using emission filters for FRET of 700–750 nm (TOB IMAGEtags; Nikon) or 660–710 nm (TOB IMAGEtags; Leica)/660–754 (6xPDC IMAGEtags; Leica) nm for the Cy5 acceptor and 560–626 nm for the Cy3 donor. To quantify the FRET signals from sensitized emission, the mean fluorescence intensities from the cells were determined by summing through the Z stack to provide pixel volumes (relative intensities). The mean fluorescence intensities for the donor and sensitized emission of the acceptor were calculated by the Leica LAS AF Lite software as Σ(Pixel volumes)/(Pixel count). FRET was determined by normalizing the sensitized emission to the donor emission ($FRET = F_{FRET}/F_{donor}$). Quantification was also done using the formula $FRET = (B - A \cdot b - c \cdot C)/C$, where B is FRET emission, A is donor emission, b is donor emission cross talk ratio (B in donor only sample/A in donor only sample), c is acceptor excitation crosstalk (B in acceptor only sample/C in acceptor only sample), ratio, C is acceptor emission (19). This latter calculation is most appropriate for application to cell studies because variations in intracellular concentrations of the two dye-labeled ligands are accounted for separately in the formula.

For FRET analysis by acceptor photobleaching, cells were grown in SD−uracil containing 2% galactose for a 30-min induction period and then incubated together with a mixture of 25 μM each of Cy3- and Cy5-tobramycin or 20 μM each of Cy3- and Cy5-PDC in SD−uracil containing 2% galactose. These concentrations and the ratios of donor to acceptor were also varied between experiments to achieve equal intracellular levels of both. For experiments in which the concentrations were different from those described here, the concentrations of ligands are stated in the legend to the figure. The cells were washed once with TBS and placed on a poly d-lysine-coated glass bottom culture dish. Acceptor bleaching was performed with a Leica SP5X laser scanning confocal microscope using the FRET acceptor bleaching wizard. Prebleach and postbleach images were taken serially with excitation of 550 nm of WLL with lower laser intensity and filters of 560–640 nm (5xTOB IMAGEtags) or 560–626 nm (6xPDC IMAGEtags) for collecting Cy3 emission and 660–710 nm (5xTOB IMAGEtags) or 660–754 nm (6xPDC IMAGEtags) for Cy5 emission. The acceptor was bleached with high laser intensity at 650 nm of WLL. The fluorescence intensities of the donor prebleach

(F_D) and postbleach (F'_D) conditions were measured by using the LAS AF Lite program. The FRET efficiencies were calculated using the formula FRET efficiency $= 1-F_D/F'_D$ (20).

Quantitative analysis of IMAGEtag transcripts by RT-qPCR

Steady-state levels of mRNAs were analyzed by quantitative reverse transcriptase-polymerase chain reaction (RT-qPCR). Yeast RNA was extracted by phenol chloroform using glass beads (21). Cells were harvested in 0.6 ml of RNA extraction buffer (10-mM ethylenediaminetetraacetic acid, 50-mM Tris-HCl pH 7.5, 0.1-M NaCl, 5% sodium dodecyl sulphate) and 0.6 ml of phenol:chloroform:isoamyl alcohol (49.5:49.5:1). After 6-min incubation at room temperature, ∼0.2 g of glass beads (0.45-mm diameter) was added and the cells were lysed by vigorous agitation for 2 min. Following centrifugation, the aqueous phase was collected; the RNA was precipitated by ethanol, dissolved in water and then treated with RNase-free DNase I (1 U/ml, Invitrogen) at 24°C for 15 min to remove traces of genomic deoxyribonucleic acid (DNA). One microgram of RNA was transcribed to create cDNA using the SuperScript III reverse transcriptase (Invitrogen) and oligo-dT as a primer in a final volume of 20 μl. After reverse transcription, 2 μl of a 1:2-diluted cDNA was used as a template for qPCR with SYBRgreen (Invitrogen) and Taq polymerase (New England BioLabs) into a final volume of 15 μl in the Opticon (Bio-Rad). The forward 4659 (AAGCTTAAAAATTTCGAGCATGCATCT) and reverse 4657 (CCTAGACTTCAGGTTGTCTAACTCC) primers were located outside the IMAGEtag sequences. The levels of galactokinase mRNA, the endogenous positive control for activity of the GAL1 promoter, were determined by PCR amplification with the forward primer 4654 (TTTGATATGCTTTGC GCCGTC) and the reverse primer 4655 (AGTCCGACACAGAAGGATCAATT). The IMAGEtag and galactokinase RNA expression levels were normalized to the ACT1 mRNA levels, which were determined in the same samples using the forward and reverse primers 4609 (ATTCTGAGGTTGCTGCTTT) and 4610 (GTCCCAGTTGGTGACAATAC), respectively. The PCR thermal cycling conditions were 5-min denaturation at 94°C; 40 cycles at 94°C for 15 s, 60°C for 15 s and 72°C for 15 s.

RESULTS

Basic strategy

Our strategy for measuring promoter activity in real-time and *in vivo* involves the use of strings of repeated RNA aptamers (IMAGEtags) that are inserted either as a synthetic coding region after a promoter of choice for plasmid-based expression or into an endogenous gene to form a fusion transcript (Figure 1). Two forms of fluorescent ligands, which constitute a FRET pair, are exogenously provided that enter the cells by passive diffusion. Binding of fluorescent ligands by the transcribed IMAGEtags is observed by way of an increased FRET signal that results from the close proximity of Cy3- and Cy5-linked aptamer ligands while they are bound to the IMAGEtags. In these studies, Cy3- and Cy5-linked aptamer ligands were used as the FRET pairs (Supplementary Figures S1–S3).

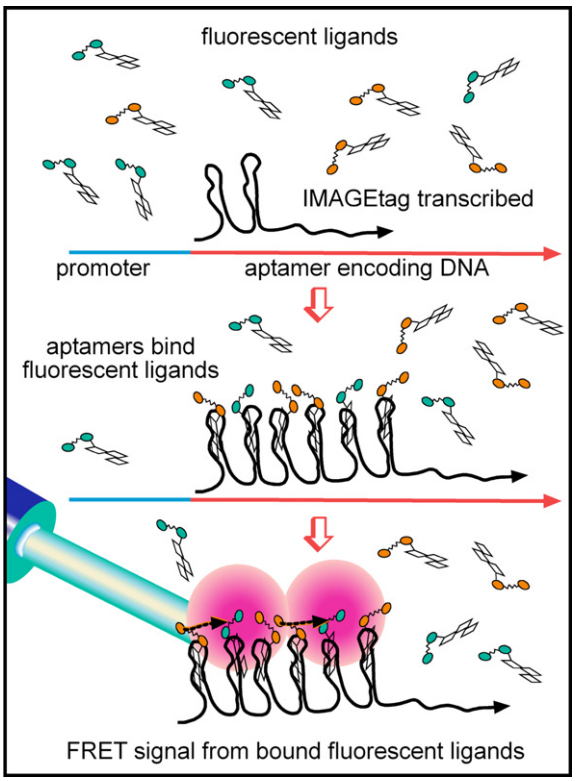

Figure 1. Schematic diagram of the IMAGEtag system. IMAGEtags (Intracellular Multiaptamer GEnetic tags) are tandemly repeated aptamers that are transcribed in the cells as an mRNA construct from a promoter of choice. IMAGEtags bind fluorescently labeled ligands that are labeled with one of the two members of a FRET pair and the bound ligands are visualized by FRET.

IMAGEtags specifically detected by FRET

Aptamers that recognize either tobramycin or PDC and derivatives (structures in Supplementary Figures S1–S3) were used in the IMAGEtag format in reporter RNAs under the control of the GAL1 promoter. In all instances when the appropriate ligands were used to visualize the expressed IMAGEtags, FRET images were obtained during the 30–80-min period after inducing the promoter with galactose (Figure 2). The number of aptamers in a string is flexible with cells expressing IMAGEtags of 5, 10 and 14 tobramycin aptamers or six PDC aptamers all giving FRET signals higher than the control RNA with no aptamers. Reduced FRET emission, such as observed in Figure 2A for the 14xTOB IMAGEtags, was associated with lower IMAGEtag RNA expression levels (Figure 2C). Incorrect binding combinations, such as Cy3-PDC and Cy5-PDC, with the 5xTOB IMAGEtags (Figure 2B and D) gave no additional signal compared with the control RNA. FRET signals, calculated as the ratio of fluorescence intensity of a FRET image to that of a donor image, were quantified from Z stacks of individual yeast cells. When incubated with the PDC ligand set, cells expressing the 6xPDC IMAGEtags showed higher FRET signals than those expressing the 5xTOB IMAGE-

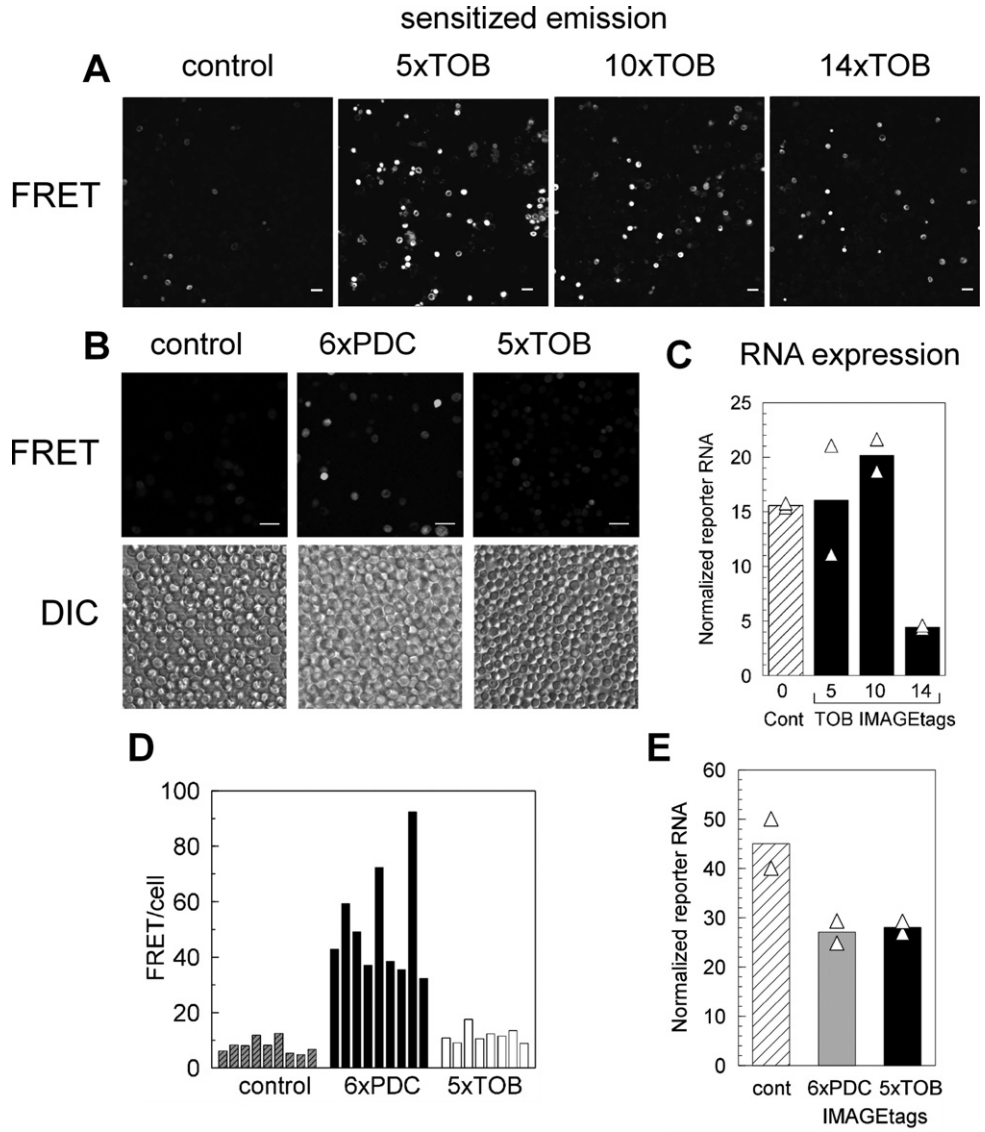

Figure 2. Analysis of IMAGEtags expressed in yeast. The FRET signal from ligand-bound IMAGEtags was detected by sensitized emission. Images of fluorescent yeast cells expressing IMAGEtags from the GAL1 promoter were obtained by confocal microscopy (**A**) and (**B**), and the differential interference contrast (DIC) images show the cells in the respective fields (B). (A) Tobramycin IMAGEtags with Cy3- and Cy5-tobramycin: cells with plasmids to express control RNA or IMAGEtags containing 5, 10 or 14 tandem tobramycin aptamers from GAL1 were induced by galactose for 1 h after overnight culture in SD−uracil with glucose and were then incubated with 25-μM Cy3-tobramycin and 25-μM Cy5-tobramycin for 20 min. Scale bar, 10 μm. (B) 6xPDC and 5xTOB IMAGEtags with Cy3- and Cy5-PDC. Cells expressing control RNA, 6xPDC or 5xTOB IMAGEtags were induced by galactose for 30 min and incubated with 5-μM Cy3-PDC and 5-μM Cy5-PDC for 30 min. (**C**) RNA expression for the experiment in (A). (**D**) Quantification of FRET from 6xPDC and 5xTOB IMAGEtags in single cells: cells were induced by galactose for 30 min and incubated with 5-μM Cy3-PDC and 5-μM Cy5-PDC for 30 min [images shown in (B)]. The fluorescence intensities of the donor and of FRET summed through the Z stack were measured from nine different cells in each field. The mean fluorescence intensity was calculated as ΣPixel volume/(Pixel count x number of slices). FRET was determined by the formula, FRET = FFRET/Fdonor. (**E**) RNA expression for experiments in (B) and (D). (C) and (E) The amount of control or IMAGEtag RNA in each population was determined in duplicate samples by RT-qPCR and each value normalized to ACT1 in the same sample. Bars, the average mRNA level (hashed bars, control RNA; grey bar, 6xPDC IMAGEtag, black bars, 5xTOB IMAGEtags). Δ: individual estimates. More images associated with this figure are in Supplementary Figures S16 and S17.

tags or the control RNA (Figure 2D). Steady-state RNA levels measured in the same cell populations for the 6xPDC IMAGEtags, 5xTOB IMAGEtags and control RNA were not correlated with the strength of the FRET signals, thus pointing to the RNA–ligand interaction as the dominant factor contributing to the FRET image (Figure 2B and D). In all instances, RNA expression was quantified for the control and IMAGEtag RNAs (Figure 2C and E).

Cell to cell variability of promoter activity

To evaluate the cell to cell variability of Pol II promoter activity in living cells, we used IMAGEtags as reporters from three promoters: GAL1, ACT1 and ADH1. FRET signals in individual cells were quantified with time after induction of the GAL1 promoter and compared with the IMAGEtag RNA levels in the same cell populations (Figure 3A–C).

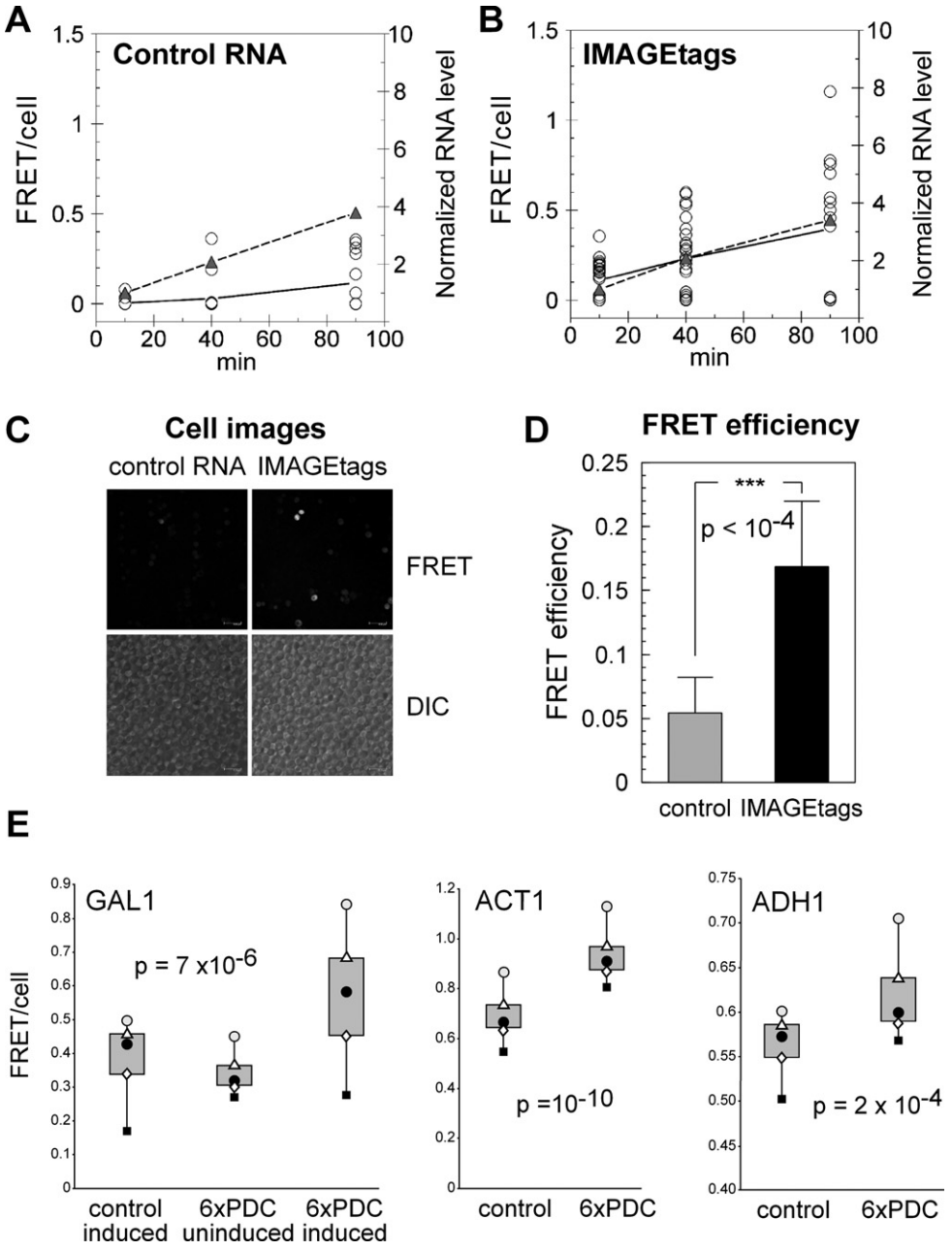

Figure 3. Time-dependent change in IMAGEtag RNA level after activation of the GAL1 promoter. Yeast cells transformed with a 2-μm plasmid for expression of control RNA (**A**) or 6xPDC IMAGEtags (**B**) both under the control of the GAL1 promoter were induced with galactose. FRET: yeast cells (n = 15–27) expressing control RNA (A) or 6xPDC IMAGEtags (B) were incubated for 90 min with 5-μM Cy3-PDC and 5-μM Cy5-PDC in medium containing 1% raffinose and no glucose. The cells were induced by the inclusion of 2% galactose for the last 10, 40 and 90 min of the incubation. The FRET values for individual cells are shown as circles and the average FRET is the uninterrupted line. The amount of IMAGEtag RNA in each population was determined by RT-qPCR and normalized to ACT1 mRNA. Fold change of RNA level indicated with a dashed line and black triangles. (**C**) Image showing FRET signals in cells with control RNA and 6xPDC IMAGEtags after 90-min induction with 2% galactose. (**D**) FRET efficiency determined by acceptor photobleaching: the average FRET efficiency from three independently performed experiments is shown with the standard deviation in error bars. ***, $P < 0.0001$. FRET efficiencies were calculated using the formula FRET efficiency = $1–F_D/F'_D$, where F_D and F'_D are donor intensity before and after photobleaching the acceptor, respectively. (**E**) Quantification of expression of IMAGEtags from three yeast promoters. 6xPDC IMAGEtags were expressed under the control of the GAL1, ACT1 or ADH1 promoters and are imaged in the presence of 10-μM Cy3-PDC and 4-μM Cy5-PDC. Box plots are shown of compiled data from experiments in which 15–20 cells were quantified for each estimate. Quantification used the formula FRET = $(B–A{\cdot}b–c{\cdot}C)/C$ described in the Materials and Methods section. P values are shown for the statistical significance of 6xPDC IMAGEtags induced versus uninduced (GAL1) or control RNA versus 6xPDC IMAGEtags (ACT1 and ADH1). •:median; ■: minimum; ◯: maximum; ◇: q1; △; q3.

Yeast cells expressing the control RNA containing no IMAGEtags (Figure 3A) or 6xPDC IMAGEtags (Figure 3B) were induced for different time periods and the FRET signal was measured in individual cells. There was a large variation in the range of individual cellular FRET signals at each time point under these conditions of preculture in glucose. However, the average increase in FRET, which represents the ensemble of induced cells, was proportional to the increase in IMAGEtag RNA level of the population measured by RT-qPCR (Figure 3A and B). This result indicates that the sampling of cells for FRET in these experiments was representative of the population and is consistent with the conclusion that the observed FRET is due to newly synthesized IMAGEtag RNA. Unlike for the IMAGEtags, the average FRET output of the control population did not increase in parallel with the mRNA content of the cell population. At each time point, the average FRET output from cells expressing the 6xPDC IMAGEtags was significantly higher than from cells expressing the control RNA ($P < 0.001$). The ability of IMAGEtags to detect the activity of two constitutive promoters, ACT1 and ADH1, was also tested (Figure 3E). The statistical significance of these results is reflected in the low P values that vary from 10^{-4} to 10^{-10}. The larger variation of FRET signal from individual cells when the promoter was GAL1 (Figure 3A–C) was associated with an experimental design in which the cells were taken directly from a glucose containing medium to one with galactose replacing glucose. The GAL1 promoter is not activated until the intracellular glucose is depleted. The cell to cell variation in time to depletion of intracellular glucose may be the basis for larger variations in cell response in this experimental design compared with others. In experiments where the cells were first cultured in raffinose to allow glucose depletion, the variations in FRET signals were much smaller with an average coefficient of variation of 15% from the compiled results from seven conditions of groups of 11–21 cells (Supplementary Figure S14).

Although FRET has the advantage of greater sensitivity due to improved signal/noise, it must be validated for potential artifacts such as bleed-through of the donor signal. Photobleaching the acceptor prevents energy transfer between donor and acceptor with a resulting increase in donor fluorescence intensity (fluorescence dequenching) that is not observed in the absence of FRET. Acceptor photobleaching was performed with cells expressing 5xTOB or 6xPDC IMAGEtags or the control RNA (Figure 3D). The donor fluorescence intensity was observed to selectively increase in the IMAGEtag expressing cells after acceptor photobleaching and the calculated FRET efficiency was higher in IMAGEtag expressing cells than control cells.

Real-time measurement of promoter activity

The ability of the IMAGEtags to report changes in gene expression in real time was evaluated by tracking the sensitized FRET emission in single cells over a long time period. These experiments were designed to both monitor transcription in real time and test the association between IMAGEtag RNA levels, GAL1 promoter activation and the FRET response. To avoid the possibility that the immediacy of cell manipulation might influence the observed changes, the cells were moved directly from glucose to raffinose containing medium simultaneously with the addition of galactose. With this protocol there is a lag in GAL1 activation due to the need for the cells to first deplete their intracellular glucose stores. If IMAGEtag expression is driven by GAL1 and if the FRET emission is from IMAGEtags, then all measures of transcription from the GAL1 promoter should show the same period of lag before increasing in response to the added galactose. This result was observed and the time lags between galactose addition and FRET, IMAGEtag RNA (exogenous promoter) and galactokinase RNA (endogenous promoter) were the same (Figure 4 and Supplementary Figures S6–S7).

DISCUSSION

As RNA reporters that enable live-cell imaging of polymerase II activity, IMAGEtags provide several advantages over currently available RNA reporter systems of which the MS2 system and Spinach RNAs are the most prominent. In the MS2 system, target mRNA is recognized by the accumulation of fluorescent fusion proteins over the tagged mRNA (6,7) while in the Spinach system an aptamer stabilizes the structure of the GFP fluorophore to enable a fluorescent output (11). The MS2 system has been successfully used to localize mRNAs in yeast and mammalian cells for real-time observation of gene expression and to follow an mRNA as it traffics through the cell (6,7). However, this system involves redistribution of signal within the cell with no change in signal per cell upon increased gene expression. The MS2 system also requires stable expression of the RNA-binding fluorescent fusion proteins as well as the reporter RNA, which limits its broad applicability. The requirement to express one or more proteins for MS2-based imaging also creates a metabolic burden for the cells that could have unintended impacts on cellular activities including those that might affect the transcriptional event that is monitored (22,23). Although technologies for imaging mRNA synthesis are likely to always have some footprint on the cell, it should be minimal. The IMAGEtags are much shorter-lived than reporter proteins and other mRNAs (Supplementary Figure S8), which will allow them to be used to image gene expression as it declines as well as when it increases such as shown here. IMAGEtags also appear not to impose a metabolic burden on the cells or to change basal transcription as is evident from the lack of effect of IMAGEtag expression on yeast cell proliferation profiles and actin gene expression levels (Supplementary Figure S13).

Apart from the use of an RNA–ligand combination compared with an RNA–protein reporter combination for visualizing gene expression, the other significant difference between the MS2-GFP system and IMAGEtags is that the former does not involve an increase in signal from a cell when the reporter is expressed. Instead, the MS2-GFP system relies on the redistribution of GFP signal through the cell to localize the reporter RNA. By contrast, the change in FRET signal from a cell with IMAGEtag reporters allows determination of the average number of transcriptional events per cell per time. Because the aptamers are short, the time period before a signal is observed is also short. With an estimated transcriptional elongation rate of

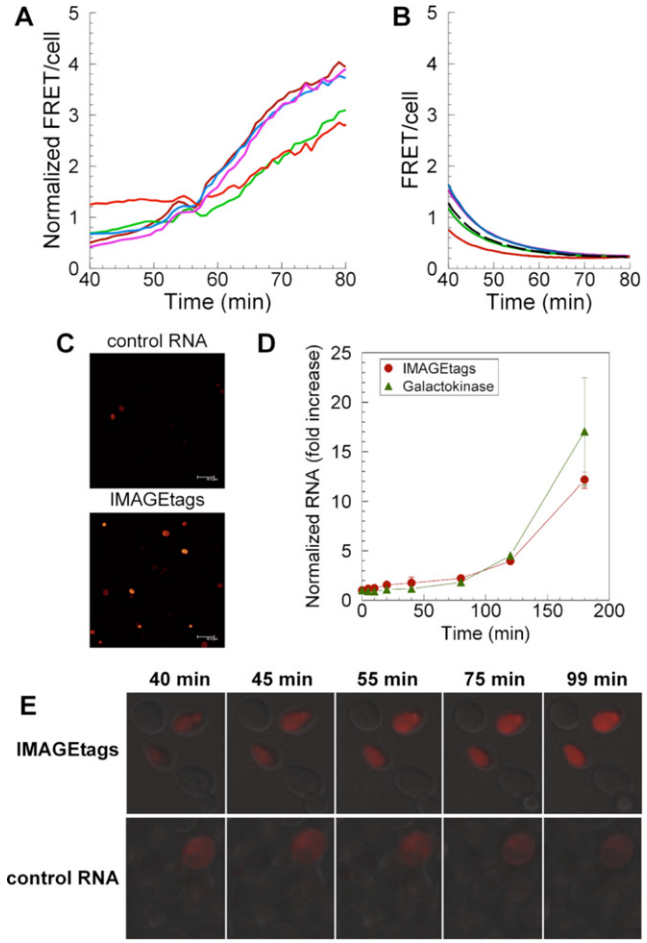

Figure 4. Real-time analysis of FRET upon induction of the GAL1 promoter. (**A**) Yeast cells containing 6xPDC IMAGEtags downstream from the GAL1 promoter were preincubated with 5-μM Cy3-PDC and 5-μM Cy5-PDC in SD−uracil with 2% galactose for 40 min. Cells were washed and resuspended in SD−uracil medium with 2% galactose and imaged by confocal microscopy for 50 min at 51-s intervals. FRET signals from individual cells expressing the 6xPDC IMAGEtags were normalized with that of the average values for control cells. (**B**) The decay of fluorescence of the control cells due to photobleaching. Decay curves are shown for four control cells and the average of these four is shown as a dashed line. These latter data were used to normalize the FRET output shown in (A). (**C**) Images 75 min after adding galactose are shown of cells expressing the control RNA or 6xPDC IMAGEtags. (**D**) Time courses of 6xPDC IMAGEtag RNA and endogenous galactokinase mRNA after induction by 2% galactose. RNA was quantified by RT-qPCR and is represented as fold increase over the 0-time measurement. All points have associated errors that are smaller than or equal to the size of the symbols if they are not seen represented by error bars. (**E**) Overlays of FRET images and DIC images of several cells during a time course of 100 min after the addition of 2% galactose to cells that had been previously incubated in 2% raffinose for 12 h.

40 nt/s (24), a delay of about 5 s is anticipated before the IMAGEtag RNAs (∼200 nt long) would produce a FRET signal. Although this report shows that IMAGEtags can be used to detect changes in transcriptional activity per cell, these reporters are also amenable to tracking locations of individual RNAs as is accomplished with the MS2-GFP system. For this application, the IMAGEtag RNA reporter should be integrated into the genome for a point source of reporter RNA in the cell as has been done for the MS2-GFP system.

Spinach RNA is an aptamer tag that was successfully used to track ribosomal RNA (rRNA) through cells (11). However, far more 5S rRNA is transcribed by Pol III than any mRNA product of Pol II. Thus, for imaging mRNA expression in real time the challenge is to obtain a high signal-to-noise ratio from an RNA tag. We have tested the Spinach RNA tag in the yeast system for its ability to report on the synthesis of a Pol III 5S rRNA product and an mRNA expressed from the GAL1 promoter. Although we saw no signal above background for the Pol II-driven transcription, we observed a significant signal from cells expressing the Spinach RNA under the control of the 5S promoter [Supplementary Figures S10–S13; (11)]. The latter result is consistent with those of the previous report (11). As for the Spinach ligand, the IMAGEtag ligands are not toxic to the cells in the time frames of our current experiments. But, unlike Spinach, IMAGEtags utilize FRET for high signal/noise to provide high sensitivity. Light-activated molecular beacons have been reported with a FRET output and nanoflares with light activated fluorescent output, but these probes allow only transient monitoring, require transfection for their delivery and are useful to image steady-state levels of RNAs rather than transcriptional activity (25,26).

As for all RNA tags, IMAGEtags must be evaluated for their possible effects on RNA metabolism and cell function before they are used for tracking transcription or RNA localization. In some studies, RNA tags did not affect the steady-state levels, regulation or processing of the RNA in which they were embedded (27,28) and in other studies the embedded tags did not affect the cell growth characteristics (28–33). However, some studies have shown that the position of the tag in the RNA, and/or its sequence context, altered the RNA steady-state expression level (34,35). Steady-state levels result from the sum of transcription, processing and degradation rates, and we are unaware of studies to determine if the reported differences in steady-state levels of RNAs containing tags, compared with no tags or tags embedded in a different position in the RNA, are due to changes in transcription rates. However, these observations of effects of the tags on steady-state RNA levels reinforce the importance of preliminary studies to establish that the embedded aptamers do not affect the molecular process under investigation or the physiology of the cells.

At least two adjacent aptamers are required to achieve a FRET signal from IMAGEtags which must each fold appropriately to bind the ligand. RNA folding and ligand affinity can vary greatly with the ionic environment and is not always accurately predicted by current folding algorithms (36). Although we used *in vitro* analysis of IMAGEtag to ligand binding (Supplementary Figure S5) and predictions of RNA folding (Supplementary Figure S18) to guide us in developing the IMAGEtags, we eventually concluded that the best test of their efficacy was to determine if these RNA reporters would function in a living cell. The ability of an aptamer to participate in a string as part of an IMAGEtag does not seem to be rare. Four of the five different aptamers that we developed into IMAGtags and tested in cells demonstrated function. The results

of two (tobramycin and PDC) are demonstrated here. Two others (the malachite green and neomycin aptamers) also demonstrated reporter activity, whereas theophylline aptamer strings were not found to be functional. In each case, a 4-base linker (A_4) separated the aptamers in the IMAGEtag. Another consideration for IMAGEtag design was how many aptamers should be present per aptamer string. A string of four or more aptamers of the same type is expected to give at least 75% of the FRET signal of perfectly alternating FRET pairs. We tested a series of lengths of aptamers (5, 10 and 14) in our preliminary trials such as shown for the tobramycin IMAGEtags (Figure 2A). All provided a good signal with similar FRET efficiencies per cell (Supplementary Figure S15). The steady-state expression level of the 5XTOB IMAGEtag was the most reproducible, perhaps due to experimental variation or to a more fundamental reason such as different RNA degradation rates for the different IMAGEtag lengths.

The ligand characteristics are also an important consideration for choosing the aptamers to be included in IMAGEtag. For example, although we found that the malachite green aptamer produced a functional IMAGEtag (data not shown), all analogs of malachite green were highly toxic to yeast and mammalian cells (17). By contrast, the tobramycin and PDC ligands used here were not toxic after 4-h incubation with the cells (Supplementary Figure S3). Another important characteristic is the ability of the ligands to enter and leave the cells freely. The intracellular concentrations of both ligands should be similar and in the range of the dissociation constant (K_d) of the aptamers in the IMAGEtag reporter. To approximate the intracellular environment, our *in vitro* K_d measurements were made using a buffer designed to reproduce the intracellular cation concentrations (Supplementary Figure S5 and Supplementary Table S1). To account for cell permeability of different ligands such as PDC and tobramycin, the former being more permeable, we quantified the steady-state levels of fluorescence from the donors and acceptors of each type in cells incubated for at least 4 h with the respective ligands. Performance of the IMAGEtags was also tested empirically with different concentrations of extracellular ligand of each type to optimize IMAGEtag reporting.

IMAGEtags can readily be attached to any RNA and used as reporters from transiently transfected cells. Compared with the more complicated procedures required to analyze images that are created by the aggregation of fluorescent proteins on a background of the same signal, we were able to obtain statistically significant results using standard sensitized FRET and acceptor photobleaching measurements and calculations. Thus, the IMAGEtags provide a generally applicable means of studying gene expression in living cells and in real time. They also have the advantage that they do not require oxygen to generate the signal and thus can be used to track promoter activity under anaerobic conditions.

Previous comparisons of cell signal transmission and activation of gene expression have identified large variations in activity between individual cells (7,37). Consequently, we analyzed the variability among cells in FRET signals from the background (control RNA), constitutive promoter (ACT1) and galactose-induced GAL1 promoter under two conditions of preculture (Supplementary Figure S14). From these studies we conclude that the relative variability in FRET of cells expressing the IMAGEtags in response to activation by galactose is mostly due to the experimental design and involved the method of preparation of the cells. In cell populations that were precultured in raffinose the variation in FRET response from GAL1 promoter IMAGEtag reporters was about the same as for the constitutive promoters and with an average of 15% coefficient of variation for all populations tested, whereas it was higher if the cells were moved directly from glucose to galactose.

CONCLUSION

The IMAGEtag method, based on a FRET signal from transcribed reporter RNAs and fluorescently modified ligands, enables live-cell imaging of polymerase II transcriptional activity in real time. Compared with the current imaging systems that rely on fluorescent proteins, these RNA reporters are a significantly lower metabolic burden for the cells that are imaged and do not accumulate in the cells. Consequently, IMAGEtags are expected to have minimal or no impact on cell behavior. The IMAGEtags system can also be expressed from plasmids in transient transfection experiments without the need to genetically modify the host cells. This system for non-invasive tracking of gene expression in real time will be especially useful for studying gene expression that changes rapidly such as during cell differentiation and in development due to external soluble factors, when cells contact others or when they encounter a change in the nature of the substratum that they are traversing.

SUPPLEMENTARY DATA

Supplementary Data are available at NAR Online, including [1–9].

ACKNOWLEDGMENTS

We thank Aditi Agrawal for help with Spinach cloning, Dr Tianjiao Wang for the RNA folding images and Margie Carter in the ISU Confocal Microscopy and Multiphoton Facility for help with fluorescence microscopy. We also thank Eirik Haarberg for early work on designing vectors and modifying the method for cloning multiple aptamers.

FUNDING

The National Institute of Health funded the developmentof the IMAGEtags (R01 EB005075), and selection and optimization of the PDC aptamer (R43 CA-110222). The U.S. Department of Energy, Office of Biological and Environmental Research through the Ames Laboratory funded the implementation of the IMAGEtags in yeast. The Ames Laboratory is operated for the U.S. Department of Energy by Iowa State University under Contract No. DE-AC02-07CH11358. Funding for open access charge: Ames Laboratories, US Department of Energy.

Conflict of interest statement. Marit Nilsen-Hamilton owns Molecular Express Inc. that provided the PDC aptamer.

REFERENCES

1. Endoh,T., Mie,M. and Kobatake,E. (2008) Direct detection of RNA transcription by FRET imaging using fluorescent protein probe. *J. Biotechnol.*, **133**, 413–417.
2. Liu,H.S., Jan,M.S., Chou,C.K., Chen,P.H. and Ke,N.J. (1999) Is green fluorescent protein toxic to the living cells? *Biochem. Biophys. Res. Commun.*, **260**, 712–717.
3. Koelsch,K.A., Wang,Y., Maier-Moore,J.S., Sawalha,A.H. and Wren,J.D. (2013) GFP affects human T cell activation and cytokine production following in vitro stimulation. *PLoS ONE*, **8**, e50068.
4. Hanazono,Y., Yu,J.M., Dunbar,C.E. and Emmons,R.V. (1997) Green fluorescent protein retroviral vectors: low titer and high recombination frequency suggest a selective disadvantage. *Hum. Gene Ther.*, **8**, 1313–1319.
5. Close,D.M., Ripp,S. and Sayler,G.S. (2009) Reporter proteins in whole-cell optical bioreporter detection systems, biosensor integrations, and biosensing applications. *Sensors*, **9**, 9147–9174.
6. Bertrand,E., Chartrand,P., Schaefer,M., Shenoy,S.M., Singer,R.H. and Long,R.M. (1998) Localization of ASH1 mRNA particles in living yeast. *Mol. Cell*, **2**, 437–445.
7. Larson,D.R., Zenklusen,D., Wu,B., Chao,J.A. and Singer,R.H. (2011) Real-time observation of transcription initiation and elongation on an endogenous yeast gene. *Science*, **332**, 475–478.
8. Hocine,S., Raymond,P., Zenklusen,D., Chao,J.A. and Singer,R.H. (2013) Single-molecule analysis of gene expression using two-color RNA labeling in live yeast. *Nat. Methods*, **10**, 119–121.
9. Valencia-Burton,M., McCullough,R.M., Cantor,C.R. and Broude,N.E. (2007) RNA visualization in live bacterial cells using fluorescent protein complementation. *Nat. Methods*, **4**, 421–427.
10. Yamada,T., Yoshimura,H., Inaguma,A. and Ozawa,T. (2011) Visualization of nonengineered single mRNAs in living cells using genetically encoded fluorescent probes. *Anal. Chem.*, **83**, 5708–5714.
11. Paige,J.S., Wu,K.Y. and Jaffrey,S.R. (2011) RNA mimics of green fluorescent protein. *Science*, **333**, 642–646.
12. Auffinger,P., Grover,N. and Westhof,E. (2011) Metal ion binding to RNA. *Met. Ions Life Sci.*, **9**, 1–35.
13. Christian,J.H. and Waltho,J.A. (1961) The sodium and potassium content of non-halophilic bacteria in relation to salt tolerance. *J. Gen. Microbiol.*, **25**, 97–102.
14. Csonka,L.N. (1989) Physiological and genetic responses of bacteria to osmotic stress. *Microbiol. Rev.*, **53**, 121–147.
15. Grubbs,R.D. (2002) Intracellular magnesium and magnesium buffering. *Biometals*, **15**, 251–259.
16. Romani,A. (2007) Regulation of magnesium homeostasis and transport in mammalian cells. *Arch. Biochem. Biophys.*, **458**, 90–102.
17. Kraus,G.A., Gupta,V., Mokhtarian,M., Mehanovic,S. and Nilsen-Hamilton,M. (2010) New effective inhibitors of the Abelson kinase. *Bioorg. Med. Chem.*, **18**, 6316–6321.
18. Amberg,D.C., Burke,D. J. and Strathern,J. N. (2005) High Efficiency Transformation of Yeast. *Methods Yeast Genet*, 109–112.
19. Wouters,F.S., Verveer,P.J. and Bastiaens,P.I. (2001) Imaging biochemistry inside cells. *Trends Cell Biol.*, **11**, 203–211.
20. Bhaumik,S.R. (2006) Analysis of in vivo targets of transcriptional activators by fluorescence resonance energy transfer. *Methods*, **40**, 353–359.
21. Del Aguila,E.M., Dutra,M.B., Silva,J.T. and Paschoalin,V.M. (2005) Comparing protocols for preparation of DNA-free total yeast RNA suitable for RT-PCR. *BMC Mol. Biol.*, **6**, 9.
22. Heyland,J., Blank,L.M. and Schmid,A. (2011) Quantification of metabolic limitations during recombinant protein production in Escherichia coli. *J. Biotechnol.*, **155**, 178–184.
23. Heyland,J., Fu,J., Blank,L.M. and Schmid,A. (2011) Carbon metabolism limits recombinant protein production in Pichia pastoris. *Biotechnol. Bioeng.*, **108**, 1942–1953.
24. Kos,M. and Tollervey,D. (2010) Yeast pre-rRNA processing and modification occur cotranscriptionally. *Mol. Cell*, **37**, 809–820.
25. Prigodich,A.E., Randeria,P.S., Briley,W.E., Kim,N.J., Daniel,W.L., Giljohann,D.A. and Mirkin,C.A. (2012) Multiplexed nanoflares: mRNA detection in live cells. *Anal. Chem.*, **84**, 2062–2066.
26. Qiu,L., Wu,C., You,M., Han,D., Chen,T., Zhu,G., Jiang,J., Yu,R. and Tan,W. (2013) A targeted, self-delivered, and photocontrolled molecular beacon for mRNA detection in living cells. *J. Am. Chem. Soc.*, **135**, 12952–12955.
27. Meitert,J., Aram,R., Wiesemann,K., Weigand,J.E. and Suess,B. (2013) Monitoring the expression level of coding and non-coding RNAs using a TetR inducing aptamer tag. *Bioorg. Med. Chem.*, **21**, 6233–6238.
28. Srisawat,C. and Engelke,D.R. (2001) Streptavidin aptamers: affinity tags for the study of RNAs and ribonucleoproteins. *RNA*, **7**, 632–641.
29. Barberis,M., Beck,C., Amoussouvi,A., Schreiber,G., Diener,C., Herrmann,A. and Klipp,E. (2011) A low number of SIC1 mRNA molecules ensures a low noise level in cell cycle progression of budding yeast. *Mol. Biosyst.*, **7**, 2804–2812.
30. Daigle,N. and Ellenberg,J. (2007) LambdaN-GFP: an RNA reporter system for live-cell imaging. *Nat. Methods*, **4**, 633–636.
31. Grate,D. and Wilson,C. (2001) Inducible regulation of the S. cerevisiae cell cycle mediated by an RNA aptamer-ligand complex. *Bioorg. Med. Chem.*, **9**, 2565–2570.
32. Haim-Vilmovsky,L., Gadir,N., Herbst,R.H. and Gerst,J.E. (2011) A genomic integration method for the simultaneous visualization of endogenous mRNAs and their translation products in living yeast. *RNA*, **17**, 2249–2255.
33. Vasudevan,S. and Steitz,J.A. (2007) AU-rich-element-mediated upregulation of translation by FXR1 and Argonaute 2. *Cell*, **128**, 1105–1118.
34. Said,N., Rieder,R., Hurwitz,R., Deckert,J., Urlaub,H. and Vogel,J. (2009) In vivo expression and purification of aptamer-tagged small RNA regulators. *Nucleic Acids Res.*, **37**, e133.
35. Hogg,J.R. and Collins,K. (2007) RNA-based affinity purification reveals 7SK RNPs with distinct composition and regulation. *RNA*, **13**, 868–880.
36. Ilgu,M., Wang,T., Lamm,M.H. and Nilsen-Hamilton,M. (2013) Investigating the malleability of RNA aptamers. *Methods.*, **6**, 178–187.
37. Rajan,S., Djambazian,H., Dang,H.C., Sladek,R. and Hudson,T.J. (2011) The living microarray: a high-throughput platform for measuring transcription dynamics in single cells. *BMC Genomics*, **12**, 115.